Appl. Phys. B 72, 121–125 (2001) / Digital Object Identifier (DOI) 10.1007/s003400000509

Applied Physics B
Lasers
and Optics

Isotopic ratio measurement of methane in ambient air using mid-infrared cavity leak-out spectroscopy

H. Dahnke[1], **D. Kleine**[1], **W. Urban**[2], **P. Hering**[1], **M. Mürtz**[1,*]

[1] Institut für Lasermedizin, Universität Düsseldorf, 40225 Düsseldorf, Germany
[2] Institut für Angewandte Physik, Universität Bonn, 53115 Bonn, Germany

Received: 14 July 2000 /Revised version: 25 October 2000/Published online: 6 December 2000 –

Abstract. We report on infrared laser spectroscopic measurements of the isotopic composition of methane ($^{12}CH_4$, $^{13}CH_4$) in natural air samples with a cavity ring-down technique. A CO overtone sideband laser is utilized to excite a high-finesse cavity which provides an effective optical absorption path length of 3.6 km. We achieved a detection limit of 105 ppt methane in ambient air using an integration time of 20 s. This corresponds to a minimum detectable absorption of 1.9×10^{-9} /cm. Rapid determination of the $^{13}C/^{12}C$ isotopic ratio of methane in ambient air without sample preconcentration or gas processing is realized. The present system requires only few minutes for an isotopic ratio measurement with a precision of 11‰ .

PACS: 07.88.+y; 42.62.Fi; 07.57.Ty

The greenhouse gas methane is the most abundant hydrocarbon in the atmosphere. Within the last 300 years its average fraction in the atmosphere has risen from 0.8 to 1.7 ppm and is still increasing [1, 2]. As regards importance for global warming, it ranks second after carbon dioxide, since a methane molecule has a 20 year integrated global warming potential, which is about 23 times that of a carbon dioxide molecule [3]. Methane also plays an important role in complex feedback mechanisms in tropospheric and stratospheric chemistry [4]. These facts indicate the importance of accurate knowledge about the sources of atmospheric methane. The measurement of the abundance of the stable isotopes is widely perceived as a key for understanding the sources and sinks of methane in the atmosphere. It can be used to estimate the relative source strength of the diverse biogenic and geochemical as well as anthropogenic sources of methane and their variation with time [5]. Next to the main isotopomer $^{12}CH_4$ (98.8%), one finds about 1.1% of $^{13}CH_4$ [6]. For example, emissions caused by biomass burning are enriched in ^{13}C as compared to the average atmospheric amount. Other sources can also be characterized by their $^{13}CH_4/^{12}CH_4$ ratio, like rice fields or the rumen of cattle [4]. The ratio is expressed by the value of $\delta^{13}C$, which is defined as

$$\delta^{13}C = \left(\frac{\left(^{13}C/^{12}C\right)_{\text{sample}}}{\left(^{13}C/^{12}C\right)_{\text{PDB}}} - 1 \right) \cdot 1000 \,, \qquad (1)$$

where $\left(^{13}C/^{12}C\right)_{\text{PDB}} = 1.1237\%$ is the international reference value. The $\delta^{13}C$ value of different methane sinks and sources varies from $-10‰$ to $-80‰$ [4].

Isotopic measurements of atmospheric air samples are usually performed with mass spectrometry (MS), sometimes in combination with gas chromatography (GCMS). This technique provides high precision, typically $\Delta\delta^{13}C = 0.1‰ - 1‰$. However, such measurements require a large amount of gas (>100 l) and a time consuming gas processing of the air sample, which limits the quantity of available data on $\delta^{13}C$ of methane.

Spectroscopic monitoring of methane mixing ratios in natural air samples has been demonstrated several times [7–10]. Usually, infrared laser absorption spectroscopy is used in combination with a multipass cell and frequency-modulation techniques. To our knowledge, the only spectroscopic measurement of $^{13}CH_4/^{12}CH_4$ ratios in natural air far from local methane sources was published in [9]. They achieved a precision of $\Delta\delta^{13}C = \pm 44‰$.

Cavity ring-down spectroscopy (CRDS) with cw lasers is a unique tool for trace gas detection because it combines high sensitivity and a fast response [11, 12]. Compared to the conventional CRDS scheme with pulsed lasers, the cw approach has the advantage of a higher spectral resolution. Moreover, it allows the use of low-power cw laser sources, since the fraction of laser light transmitted through the ring-down cell is orders of magnitude higher. We have previously demonstrated a variant of this technique: the detection of trace gases via mid-infrared cavity leak-out spectroscopy (CALOS) [13]. Recently, we proved that this technique, applied to the 3 μm wavelength region, is sufficiently sensitive to measure the rare

*Corresponding author.
(Fax: +49-211/811-1374, E-mail: muertz@uni-duesseldorf.de)

$^{13}CH_4$ methane isotopomer in natural air [14]. The 3 μm region is ideally suited, since methane shows a characteristic fingerprint and the number of interfering lines of other atmospheric components is sufficiently low.

In this paper we report the application of CALOS in order to determine the $^{13}CH_4/^{12}CH_4$ isotopic ratio in ambient air. This was achieved without any gas processing or accumulation of the rare isotopomer and reveals the possibilities for our fast and sensitive detection method combined with easy gas handling compared to the conventional MS procedure.

1 Experiment

1.1 Cavity leak-out spectrometer

The experiments were performed using a CO overtone laser that operates on about 300 rovibrational $\Delta v = 2$ transitions in the wavelength region between 2.6 and 4.1 μm with single line output power on the order of 100 mW [15]. By mixing the laser light with microwave radiation in an electro-optic modulator, tunable laser sidebands are generated. More details can be found in [16].

Figure 1 shows a schematic of the spectrometer. The laser consists of a liquid-nitrogen cooled gain tube which is filled with a mixture of He, N_2, CO, and air. The resonator is formed by a reflection grating in Littrow mount and an output coupler ($R = 98\%$), mounted upon a piezoelectric transducer (PZT) to achieve fine frequency control. In heterodyne experiments the spectral linewidth of the laser has been determined to be 100 kHz for an observation interval of 1 s [16, 17]. The laser light is focused into a CdTe electro-optic modulator (EOM) which generates tunable microwave sidebands covering a spectral range of 8 to 18 GHz above and below each laser line. The EOM is placed between two crossed Rochon polarizers. This setup provides spatial separation of the sidebands from the carrier as a result of their orthogonal polarisation. The typical power of the sidebands is 50 μW using 150 mW of infrared and 20 W of microwave power. The sideband radiation is mode matched by means of two lenses to excite the fundamental transverse mode of the ring-down cavity described in detail below. Behind the cavity, the two sidebands are separated by means of a 0.5 m Czerny–Turner monochromator. This ensures that only the sideband of interest reaches the liquid-nitrogen-cooled InSb photodiode.

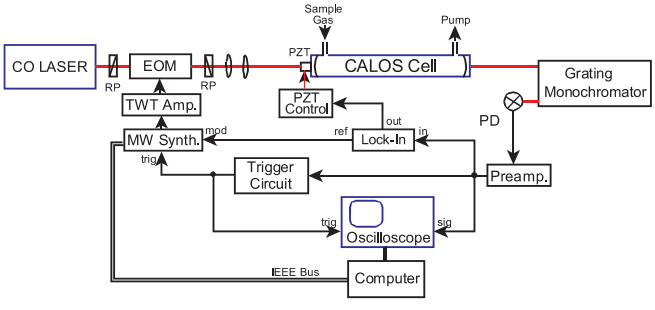

Fig. 1. Schematic of the experimental setup. PZT: Piezoceramic transducer; PD: photodiode; TWT Amp: traveling-wave tube amplifier; MW Synth.: microwave synthesizer; EOM: electro-optic modulator; RP: Rochon polarizer

1.2 Data acquisition

The CO laser frequency is sinusoidally modulated (modulation frequency: 180 Hz) via the laser PZT. First, this enables us to frequency-stabilise the laser to its gain profile maximum by means of a standard *1f* lock-in technique. Second, the laser frequency modulation allows us to frequency-stabilise a single mode of the ring-down cavity to the laser sideband of interest. This *1f* locking of the cavity to the laser is performed by controlling the cavity length via the cavity PZT (see Sect. 1.3).

The laser power is injected into the cavity twice per modulation period. Each time the laser is in the center of the cavity resonance, an increase in the transmitted power is observed (power build-up). After the photodetector signal reaches a threshold, a trigger pulse is generated which turns off the sideband power via the EOM. The power decay of the cavity field is then recorded by a digital storage oscilloscope (Tektronix TDS 620) with 8-bit vertical resolution. After averaging over 100 leak-out events, the decay signal is transferred to a personal computer. The decay time τ ($\frac{1}{e}$ time) of the leak-out signal is determined by fitting a single exponential to the data according to a nonlinear Levenberg–Marquardt algorithm. This is realized via the graphic programming language LabVIEW, which is also used to control the experiment.

The absorption coefficient α is calculated from the decay time τ as

$$\alpha = \frac{1}{c}\left(\frac{1}{\tau} - \frac{1}{\tau_0}\right), \tag{2}$$

with

$$\tau_0 = \frac{d}{c\,(1-R)}\,, \tag{3}$$

where c is the speed of light, d is the length of the cavity and R is the reflectivity of the mirrors. τ_0 is the decay time of the empty cavity showing only mirror losses.

1.3 Absorption cell and gas handling system

Figure 2 shows a schematic of the absorption cell. The cell is made of stainless steel and has two detachable end pieces. The laser beam enters and leaves the cell through antireflection-coated sapphire windows on both ends. The cavity mirrors sit on kinematic mounts inside the cell. They

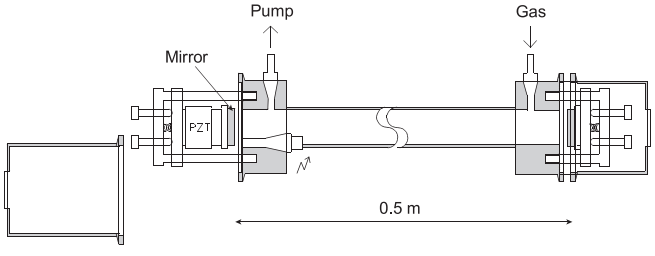

Fig. 2. Schematic of the CALOS absorption cell. The cell is made entirely of stainless steel. The PZT allows fine control of the cavity length. One of the end pieces is demounted

have a reflectivity of 99.985% around $\lambda = 3.3\,\mu$m, being of the plano-concave type with a radius of curvature of 6 m. The distance between the two mirrors is 52.5 cm, corresponding to a free spectral range (FSR) of 285.5 MHz. One of the mirrors is fixed on a PZT to allow for fine control of the cavity length.

Two gas supplies enable gas flow through the cell. In order to minimize contamination by surface-released trace gases, all parts in contact with the gas flow are made of stainless steel or Teflon. The gas flow is established by a rotary pump; the flow rate is controlled by an electronic mass flow controller to be 220 cm^3/min in standard pressure (1013 mbar) and temperature (300 K) conditions. The pressure inside the cell is kept constant at 50 mbar independently of the gas flow. This is realized via a pressure control loop consisting of a pressure transducer that supplies a control unit with the actual pressure inside the cavity and an electric valve between cell and pump driven by the pressure controller.

2 Results

2.1 Spectrum of methane in ambient air

For a measurement of the $^{13}CH_4/^{12}CH_4$ isotopic ratio, the fraction of both species in the air sample has to be determined. Therefore, characteristic absorption lines were chosen by means of the HITRAN96 database [6]. Due to the large difference in abundance of the two isotopomers these $^{13}CH_4$ spectral lines are strongly overlapped by the neighbouring spectral lines of $^{12}CH_4$. By choosing a pressure of 50 mbar, the interference of the pressure-broadened spectral lines was minimized. There are also several strong water absorption lines in the spectral region of interest which would interfere with the methane lines at higher pressure.

For the measurement of the $^{12}CH_4$ isotopomer we selected the spectral region around 2947.8 cm^{-1}, which is covered by the upper frequency sideband of the P(11), $v' - v'' = 27 - 25$, laser line. For the measurement of the $^{13}CH_4$ isotopomer we chose the spectral region around 3048.3 cm^{-1}, which can be reached with the lower frequency sideband of the P(10), $v' - v'' = 25 - 23$, laser line. The $^{13}CH_4$ spectrum in this region is relatively weakly overlapped by a $^{12}CH_4$ line which can be taken into account via subtraction of the measured $^{12}CH_4$ mixing ratio. Water lines do not significantly interfere in this region.

Figures 3 and 4 show the experimental results. The spectra were taken by scanning the microwave source in steps of 142.5 MHz. Each data point represents the mean value of ten consecutive decay time measurements which were acquired over approximately 20 s. The error bars include the uncertainty of the absorption measurement and the uncertainty of the decay time τ_0 of the empty cavity. For comparison, calculated absorption spectra of methane for a total pressure of 50 mbar are shown as solid curves in Figs. 3 and 4. This calculation is based on the line positions and pressure broadening coefficients given by the HITRAN96 database. The methane spectra obtained verify the HITRAN data for both isotopomers and reveal that there are no disturbing interferences from other atmospheric compounds.

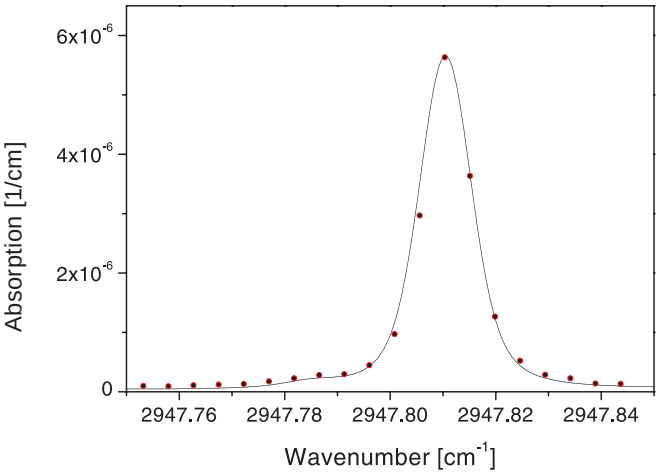

Fig. 3. Cavity leak-out spectrum of $^{12}CH_4$ in ambient air at a pressure of 50 mbar. *Dots* are experimental data. The 1σ error is below 3×10^{-8} /cm, and the corresponding error bars are smaller than the dot size. The *solid line* shows the HITRAN data for a $^{12}CH_4$ mixing ratio of 1962 ppb. The spectral line observed is the P7 E(1) 17 transition of the methane ν_3 band

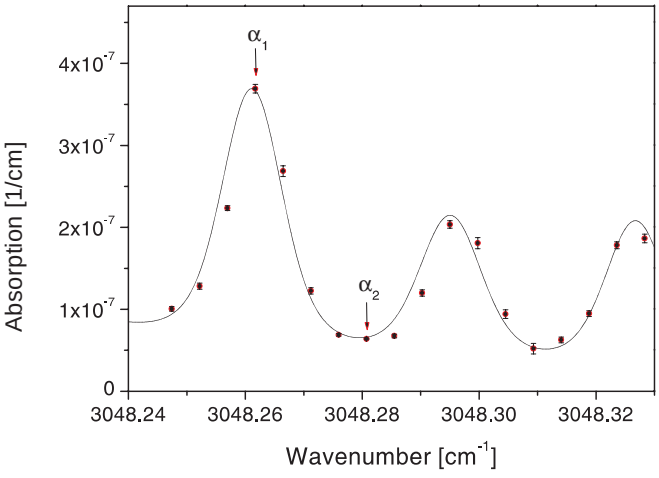

Fig. 4. Cavity leak-out spectrum of $^{13}CH_4$ in ambient air at a pressure of 50 mbar. *Dots* are experimental data. The *error bars* indicate the 1σ uncertainty in the measurements. The *solid line* shows the HITRAN data for a $^{13}CH_4$ mixing ratio of 21 ppb. Three transitions of the methane ν_3 band are observed: R3 A2(1) 1, R3 F2(1) 1, and R3 F1(1) 1. The data points marked with α_1 and α_2 were used for the determination of the $^{13}CH_4$ mixing ratio

2.2 Time resolution and sensitivity of the spectrometer

A demonstration of the spectrometer's time resolution is given in Fig. 5, where the methane fraction observed is plotted versus time. After switching from a sample gas mixture (28 ppb methane in nitrogen) to pure nitrogen, the absorption signal responds within a few seconds. The gas flow rate is 220 cm^3/min in standard pressure and temperature conditions. Considering the volume of the ring-down cell (ca. 1 l) and the pressure inside the cell (50 mbar), the time needed to exchange the gas volume of the cell was calculated to be about 13 s, which agrees reasonably well with the response curve depicted in Fig. 5.

In order to determine the detection limit of the spectrometer, we prepared a gas mixture of 209 ppt $^{13}CH_4$ by mixing

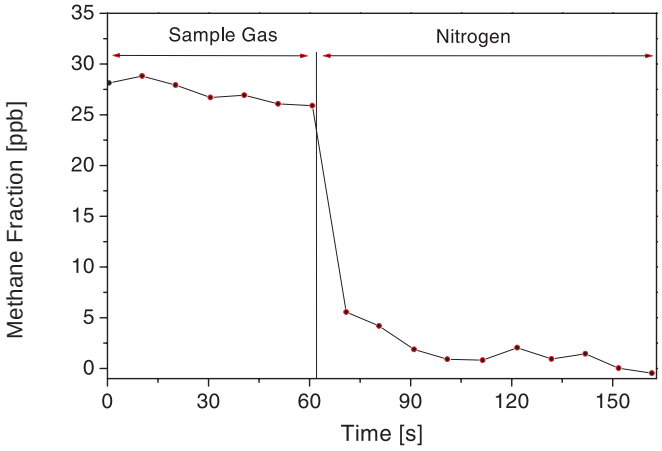

Fig. 5. Demonstration of the temporal resolution of the spectrometer. The sample gas mixture consists of 28 ppb methane in grade 5 nitrogen. The signal decay time is determined by the gas exchange time of the absorption cell volume

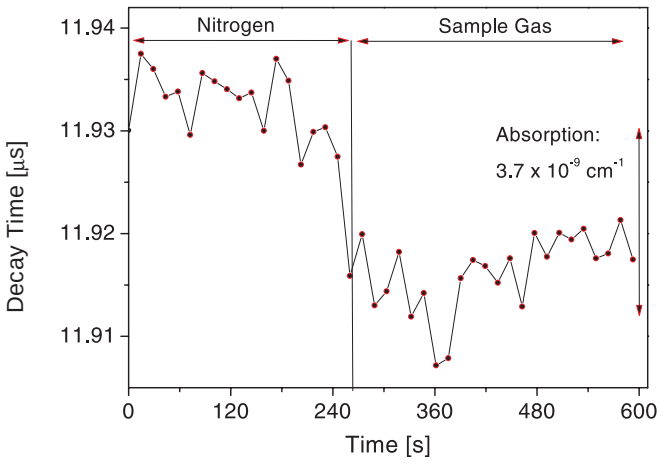

Fig. 6. Demonstration of the sensitivity of the spectrometer. The sample gas mixture is 209 ppt methane in grade 5 nitrogen. From this measurement, the detection limit for methane in ambient air is estimated to be 105 ppt

a certified gas mixture (1.3 ppm methane in grade 5 nitrogen) which contained $^{13}CH_4$ in its natural abundance in a flow ratio of 1 : 70 with grade 5 nitrogen. This yielded a mixing ratio of 209 ppt for the $^{13}CH_4$ isotopomer. Figure 6 shows the decay times for pure grade 5 nitrogen and for the sample of 209 ppt $^{13}CH_4$. The corresponding absorption coefficient of 3.7×10^{-9} cm was observed with a signal-to-noise ratio (SNR) of 2 : 1. Thus, the detection limit for methane in ambient air is 105 ppt, corresponding to a lowest detectable absorption of 1.9×10^{-9} cm. We think that the noise of the decay time, short term as well as long term, is mainly caused by acoustical jitter of the cavity mirrors. Thus, a better acoustical isolation of the cavity may improve our current detection limit.

2.3 Determination of the $^{12}CH_4/^{13}CH_4$ *ratio*

A fast determination of the isotopic ratio was performed by absorption measurements at two different frequencies for each isotopomer: at the peak of the absorption line and at a point of low absorption between lines. For the $^{12}CH_4$ measurement 20 data points were acquired during 100 s. The absorption coefficients obtained were converted to mixing ratios using the HITRAN data at the given sample temperature and pressure. In this way, the mixing ratio of $^{12}CH_4$ in our laboratory air was determined to be 1962 ± 11 ppb. The uncertainty given represents the statistical fluctuation in the decay times, which is the major error source in this case. It should be noted that this uncertainty of our measurement is not identical with the detection limit (see Sect. 2.2).

For the exact determination of the $^{13}CH_4$ fraction, accidental changes in the empty-cavity decay time τ_0 (long-term variations) have to be taken into account. A typical value for the empty-cavity decay time is $\tau_0 = 12\,\mu s$ and the long-term variations of τ_0 may be up to $\pm 0.01\,\mu s$ under unfavorable circumstances. Therefore, changes of τ_0 were monitored during the measurement in real-time without interrupting the gas flow. τ_0 can be obtained from the measurements of the decay time τ_1 at the peak of the strongest absorption line and the decay time τ_2 between lines (see Fig. 4). For these two wavelengths positions we calculated the corresponding absorption coefficients using the HITRAN data. In the following, these calculated coefficients will be denoted $\tilde{\alpha}_1$ and $\tilde{\alpha}_2$, respectively. The ratio $\tilde{\alpha}_1/\tilde{\alpha}_2$ is independent of the methane mixing ratio. As can be seen from (2), this ratio can be expressed as

$$\frac{\tilde{\alpha}_1}{\tilde{\alpha}_2} = \frac{{\tau_1}^{-1} - {\tau_0}^{-1}}{{\tau_2}^{-1} - {\tau_0}^{-1}} \,. \tag{4}$$

This yields for the empty-cavity decay time

$$\tau_0 = \left(1 - \frac{\tilde{\alpha}_1}{\tilde{\alpha}_2}\right) \cdot \left({\tau_1}^{-1} - \frac{\tilde{\alpha}_1}{\tilde{\alpha}_2} \cdot {\tau_2}^{-1}\right)^{-1} . \tag{5}$$

In this way, changes of τ_0 which are slower than the time taken between the two measurements τ_1 and τ_2 (about 4 s) can be eliminated. Furthermore, the procedure compensates for any wavelength-independent background absorption.

The absorption coefficient at the peak of the $^{13}CH_4$ line α_1 is obtained by combining (2) and (5) to give

$$\alpha_1 = \frac{1}{c} \cdot \frac{\tilde{\alpha}_1}{\tilde{\alpha}_2 - \tilde{\alpha}_1} \cdot \left({\tau_2}^{-1} - {\tau_1}^{-1}\right) . \tag{6}$$

For the $^{13}CH_4$ measurement 25 data points were acquired during 125 s. Using the absorption coefficient given by (6), we determine the mixing ratio of $^{13}CH_4$ in our laboratory air to be 21.1 ± 0.25 ppb.

From this we calculate the $\delta^{13}C$ value of methane to be $-45 \pm 11‰$, in agreement with the expected value of $-47 \pm 2‰$, which is the normal $\delta^{13}C$ value found in the German atmosphere far from specific methane sources[18, 19].

3 Discussion and conclusion

The accuracy of our spectroscopic $\delta^{13}C$ measurement depends on the statistical error arising from the limited SNR of the spectrometer and on systematic errors introduced by the conversion of the obtained absorption coefficient to the corresponding molecular density. We used the line strength and line position values of the HITRAN catalog for this conversion. The uncertainty of the HITRAN line strength and

line position data varies very much from line to line and is not available for all transitions. The fact that we obtained the expected δ^{13}C value indicates that the HITRAN data for the transitions used are sufficiently accurate. It should be noted that the temperature of the gas sample must be accurately measured since the transitions used for the different isotopomers have different lower state energies. For example, the effect of a temperature difference of 1 K upon the absorption coefficients is equivalent to a δ^{13}C change of 5‰. Therefore we measured the temperature during the experiments with an uncertainty of ± 0.1 K.

The uncertainty of our present method is a factor of 4 smaller than previously reported spectroscopic measurements [9]. A higher accuracy than that reported here can only be achieved at present through time-consuming sample processing and the use of a state-of-the-art mass spectrometer [18].

The uncertainty of ± 11‰ does not permit tracking δ^{13}C changes in the "clean" atmosphere far from methane sources, which usually are below ± 2‰; however, it is sufficient to distinguish the isotopic signatures of different methane sources which show δ^{13}C variations between -10‰ and -80‰ .

Though the idea of cavity ring-down spectroscopy has been realized in many laboratories and several variants have been developed during the past decade, applications of these techniques to atmospheric research are rarely published. Many people are concerned about cavity mirror aging and degradation through corrosion or condensation of impurities in the gas sample. Our experience is that even after weeks of continuous flow of ambient air through the ring-down cell the cavity mirrors did not significantly degrade. This qualifies the present technique for a number of other atmospheric trace gas detection applications.

In conclusion, our work demonstrates that CALOS is well suited to the detection of very small gas fractions in ambient air and to rapid isotopic composition measurements. Though at present the accuracy achieved does not reach the accuracy of a mass spectrometer, the experiment demonstrates that a direct rapid measurement of the isotopic ratio of methane in natural air samples without requiring gas processing is possible. The instrument potentially can become portable if the CO laser is replaced by a compact, tunable solid-state laser, for example, a difference-frequency generation setup. Work along these lines is currently in progress in our laboratory.

Acknowledgements. This work is supported by the Deutsche Bundesstiftung Umwelt. H.D. acknowledges a grant from the Studienstiftung des Deutschen Volkes. We are grateful to R.F. Curl, Rice University, and J. Reuss, University of Nijmegen, for useful comments on the manuscript.

References

1. IPCC Second Assessment Report: Climate Change 1995; available at http://www.ipcc.ch
2. J.P. Kennet, K.G. Cannariato, I.L. Hendy, R.J. Behl: Science **288**, 128–133 (2000)
3. J. Lelieveld, P.J. Crutzen: Nature **355**, 339-342 (1992)
4. S.C. Tylor: In *Stable Isotopes in Ecological Research*, ed. by P.W. Rundel, J.R. Ehleringer, K.A. Nagy (Springer, New York 1988) p. 395–409
5. P.J. Crutzen: Nature **350**, 380–381 (1991)
6. HITRAN96 Database; available at http://www.hitran.com
7. P. Bergamaschi, M. Schupp, G.W. Harris: Appl. Opt. **33**, 7704–7716 (1994)
8. K.P. Petrov, S. Waltman, E.J. Dlugokencky, M. Arbore, M.M. Fejer, F.K. Tittel, L. Hollberg: Appl. Phys. B **64**, 567–572 (1997)
9. S. Waltman, K.P. Petrov, E.J. Dlugokencky, M. Arbore, M.M. Fejer, F.K. Tittel, L.W. Hollberg: Digest of the IEEE/LEOS Summer Topical Meetings 1997, p. 37–38
10. D.G. Lancaster, R. Weidner, D. Richter, F.K. Tittel, J. Limpert: Opt. Commun. **175**, 461–468 (2000)
11. K. Lehmann: U.S. Patent 5528040 (1996)
12. D. Romanini, A.A. Kachanov, N. Sadeghi, F. Stoeckel: Chem. Phys. Lett. **262**, 105 (1996)
13. M. Mürtz, B. Frech, W. Urban: Appl. Phys. B **68**, 243-249 (1999)
14. D. Kleine, H. Dahnke, W. Urban, P. Hering, M. Mürtz: Opt. Lett. **25**, 1606–1608 (2000)
15. E. Bachem, A. Dax, T. Fink, A. Weidenfeller, M. Schneider, W. Urban: Appl. Phys. B **57**, 185–191 (1993)
16. M. Mürtz, B. Frech, P. Palm, R. Lotze, W. Urban: Opt. Lett. **23**, 58–60 (1998)
17. M. Mürtz, T. Kayser, D. Kleine, S. Stry, P. Hering, W. Urban: Proc. SPIE **3758**, 53–61 (1999)
18. I. Levin, H. Glatzel-Mattheier, T. Marik, M. Cuntz, M. Schmidt: J. Geophys. Res. **104**, 3447–3456 (1999)
19. I. Levin: private communication (2000)